

A new, precise measurement of the primordial abundance of Deuterium ^{*}

Max Pettini^{1,2†} and Ryan Cooke^{1,2}

¹*Institute of Astronomy, Madingley Road, Cambridge, CB3 0HA*

²*Kavli Institute for Cosmology, Madingley Road, Cambridge, CB3 0HA*

Accepted . Received ; in original form

ABSTRACT

The metal-poor ($Z \simeq 1/100Z_{\odot}$) damped Lyman alpha system (DLA) at redshift $z_{\text{abs}} = 3.04984$ in the $z_{\text{em}} \simeq 3.030$ QSO SDSS J1419+0829 has near-ideal properties for an accurate determination of the primordial abundance of deuterium, $(\text{D}/\text{H})_{\text{p}}$. We have analysed a high-quality spectrum of this object with software specifically designed to deduce the best fitting value of D/H and to assess comprehensively the random and systematic errors affecting this determination. We find $(\text{D}/\text{H})_{\text{DLA}} = (2.535 \pm 0.05) \times 10^{-5}$ which in turn implies $\Omega_{\text{b},0}h^2 = 0.0223 \pm 0.0009$, in very good agreement with $\Omega_{\text{b},0}h^2(\text{CMB}) = 0.0222 \pm 0.0004$ deduced from the angular power spectrum of the cosmic microwave background. If the value in this DLA is indeed the true $(\text{D}/\text{H})_{\text{p}}$ produced by Big-Bang nucleosynthesis (BBN), there may be no need to invoke non-standard physics nor early astration of D to bring together $\Omega_{\text{b},0}h^2(\text{BBN})$ and $\Omega_{\text{b},0}h^2(\text{CMB})$. The scatter between most of the reported values of $(\text{D}/\text{H})_{\text{p}}$ in the literature may be due largely to unaccounted systematic errors and biases. Further progress in this area will require a homogeneous set of data comparable to those reported here and analysed in a self-consistent manner. Such an endeavour, while observationally demanding, has the potential of improving our understanding of BBN physics, including the relevant nuclear reactions, and the subsequent processing of ${}^4\text{He}$ and ${}^7\text{Li}$ through stars.

Key words: quasars: absorption lines – quasars: individual: J1419+0829 – cosmology: observations.

1 INTRODUCTION

It is well known that the relative abundances of the light elements created in the first few minutes of cosmic history depend on the product of the present-day density of baryons in units of the critical density, $\Omega_{\text{b},0}$, and h^2 , where h is the present-day value of the Hubble parameter measured in units of $100 \text{ km s}^{-1} \text{ Mpc}^{-1}$. When analysed in conjunction with the the power spectrum of temperature anisotropies of the cosmic background radiation (CMB), light element abundances can improve constraints on cosmological parameters, primarily the spectral index of primordial fluctuations (Pettini et al. 2008), and on the effective number of light fermion species, N_{eff} (e.g. Simha & Steigman 2008; Nollett & Holder 2011).

Among the elements created in Big Bang nucleosynthesis (BBN), three have been the focus of most observational efforts: ${}^4\text{He}$, D and ${}^7\text{Li}$. It is a lingering concern that D is the only one of the three whose primordial abundance is consistent, within the errors, with the value of $\Omega_{\text{b},0}h^2$ deduced from the analysis of the CMB. The poor sensitivity of the primordial abundance of ${}^4\text{He}$ to $\Omega_{\text{b},0}h^2$ requires it to be measured with a precision which may be beyond what can be realistically achieved, at least until all the sources of systematic error are fully understood (Molaro 2008; Aver, Olive & Skillman 2012). On the other hand, a satisfactory explanation for the factor of ~ 3 discrepancy between the abundances of ${}^7\text{Li}$ in the oldest stars in our Galaxy and the value expected from BBN has yet to be found (Sbordone et al. 2010; Iocco 2012; Nissen & Schuster 2012 and references therein).

Even D is not entirely without its problems. As preciently pointed out by Adams (1976), its primordial abundance is most effectively deduced from the D/H ratio in metal-poor hydrogen clouds giving rise to absorption lines

^{*} Based on observations collected at the European Organisation for Astronomical Research in the Southern Hemisphere, Chile [VLT programme ID 085.A-0109(A)].

[†] email: pettini@ast.cam.ac.uk

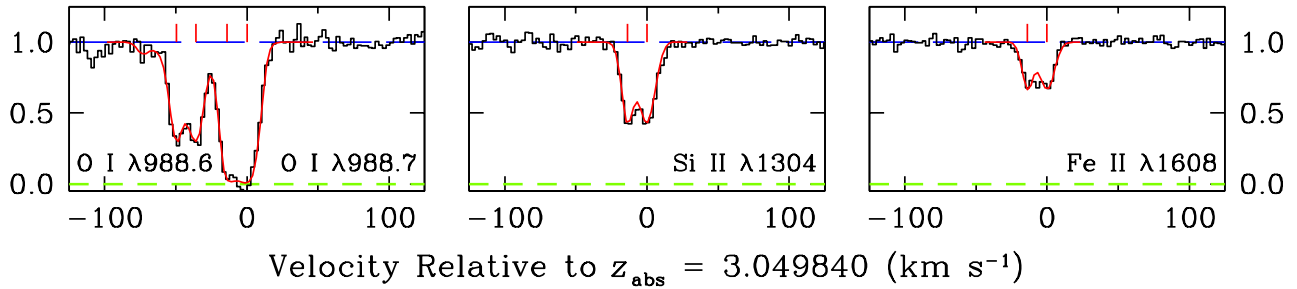


Figure 1. Selected metal lines in the $z_{\text{abs}} = 3.04984$ DLA in the QSO SDSS J1419+0829, reproduced from Cooke et al. (2011). In each panel, the black histogram is the observed spectrum and the red continuous line is the theoretical line profile fitted to the data. Vertical tick marks above the spectrum indicate the velocities of the two absorption components, with parameters listed in section 2. The y -axis scale is residual intensity. The normalized quasar continuum and zero level are shown by the blue long-dashed and green dashed lines, respectively.

in the spectra of high redshift quasars (QSOs). This is a difficult measurement, requiring not only the combined power of 8–10 m aperture optical telescopes and high resolution echelle spectrographs, but also the right combination of redshift, hydrogen column density, and internal velocity structure of the absorbing gas. Consequently, there are currently only about 10 QSO absorbers where the D I lines have been unambiguously detected free from interference from unrelated absorption. The mean value so derived, $\langle \log(D/H)_p \rangle = -4.556 \pm 0.034$ (Fumagalli et al. 2011) implies $\Omega_{\text{b},0} h^2 (\text{BBN}) = 0.0213 \pm 0.0012$ which agrees within the errors with $\Omega_{\text{b},0} h^2 (\text{CMB}) = 0.0222 \pm 0.0004$ (Keisler et al. 2011). Less satisfactory is the fact that even this prime set of D/H measures exhibits a wider dispersion about the mean than expected on the basis of the quoted errors. While the most straightforward explanation of the scatter is that systematic errors affecting some, or all, of the D/H measurements have been underestimated, more radical ideas involving early destruction of D have also been proposed (e.g. Olive et al. 2012).

Given the key role played by D in our understanding of BBN, it is important to identify and study more QSO absorbers with the optimum characteristics for the determination of the primordial D abundance $(D/H)_p$. This is the subject of the present paper.

1.1 Metal-poor damped Lyman alpha systems

Among the different classes of QSO absorbers, the so-called ‘damped Lyman alpha systems’ (DLAs) are potentially the best targets for reliable measures of $(D/H)_p$. DLAs are characterised by high column densities of neutral gas, with $N(\text{H I}) \geq 2 \times 10^{20}$ atoms cm^{-2} (Wolfe et al. 2005), and appear to be associated with galaxies at early stages of chemical evolution (Pontzen et al. 2008; Péroux et al. 2012; Krogager et al. 2012). Typical metallicities at redshifts $z = 2\text{--}4$ are $Z_{\text{DLA}} \simeq 1/10\text{--}1/100 Z_{\odot}$ (Ellison et al. 2012), but with a tail that extends to $Z_{\text{DLA}} < 1/1000 Z_{\odot}$ (Penprase et al. 2010; Cooke et al. 2011).

The number of known DLAs with metallicities less than 1/100 of solar has increased in recent years thanks to large scale sky surveys (Noterdaeme et al. 2009), and it is these systems that have proved to be choice candidates for measuring $(D/H)_p$ for the following reasons: (i) the low

metallicities imply negligible D astration (Romano et al. 2006; Prodanović et al. 2010), justifying the assumption that $(D/H)_{\text{DLA}} = (D/H)_p$; (ii) the high H I column densities result in detectable optical depths of D I absorption in *many* lines in the Lyman series. This both increases the accuracy of the measurement of $N(\text{D I})$ compared with lower column density systems, where D I absorption is detected only in the strongest Lyman lines (e.g. Burles & Tytler 1998a,b), and reduces the likelihood of contamination by unrelated absorption; (iii) the empirical correlation between metallicity and absorption line width (Murphy et al. 2007; Prochaska et al. 2008) implies that the kinematics of $Z \lesssim 1/100 Z_{\odot}$ DLAs are normally quiescent, with the absorption lines extending over a narrow velocity interval (Cooke et al. 2011). Such kinematics greatly facilitate resolving the -82 km s^{-1} isotope shift of the D I Lyman lines from the neighbouring H I absorption.

Thus, several of the very metal-poor DLAs in the recent survey by Cooke et al. (2011) are promising candidates for further observations targeting the high order D I and H I Lyman lines redshifted into the ground-base UV spectral region ($\lambda_{\text{obs}} < 4000 \text{ \AA}$). In this paper we report the analysis of what we consider to be the most suitable case in the sample by Cooke et al. (2011) for determining the primordial abundance of D with a higher precision than is normally achievable.

The paper is arranged as follows. In section 2 we briefly describe the observations (which have already been reported by Cooke et al. 2011) and summarise the most important properties of the DLA. Sections 3 and 4 are devoted to the derivation of the D/H ratio and its error, respectively. In section 5 we examine the cosmological implications which follow if the value of D/H deduced here is indeed the best measure of the primordial abundance of deuterium. We comment on earlier measurements of $(D/H)_p$ in section 6, before concluding in section 7.

2 OBSERVATIONS AND DATA REDUCTION

The spectrum of the $g = 18.9$ mag QSO SDSS J1419+0829 at $z_{\text{em}} \simeq 3.030$ shows a damped Lyman alpha system at $z_{\text{abs}} = 3.04984$; the small redshift difference between Ly α emission and absorption results in an unusually ‘clean’ Ly α absorption profile, with a red wing which is essentially free

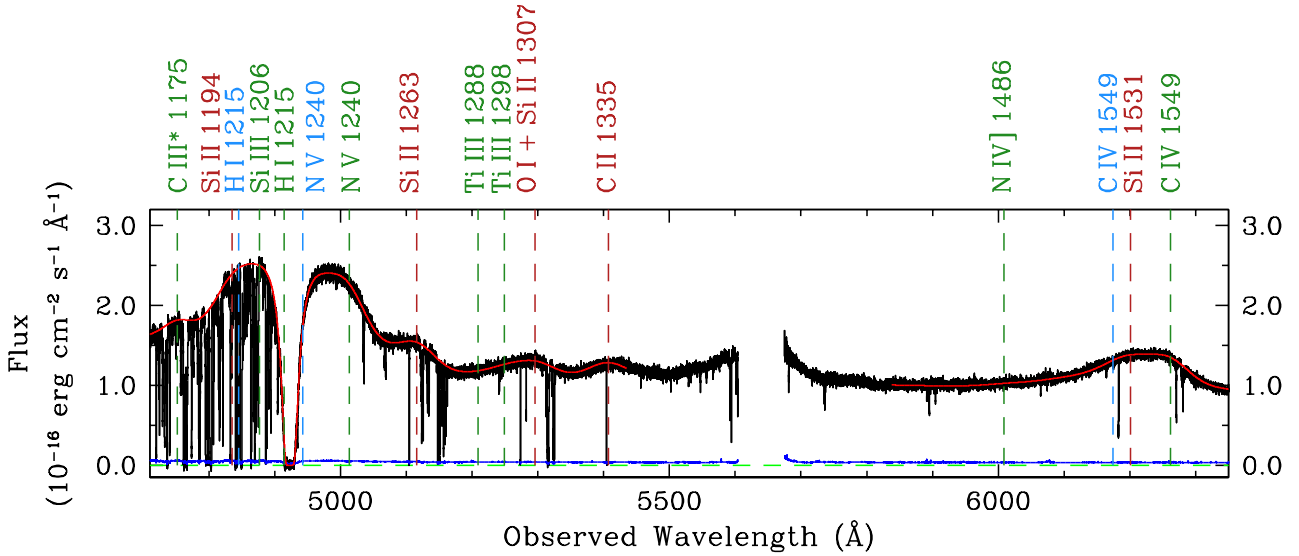


Figure 2. Portion of the UVES spectrum of the QSO SDSS J1419+0829 (black), together with the model fit (red). The 1σ error spectrum is shown in blue (near the zero level). Vertical dash lines mark the positions of QSO spectral features, as indicated. Light blue labels denote emission lines at $z_{\text{em}} = 2.98576$, green labels emission lines at $z_{\text{em}} = 3.04224$, and red labels emission lines at $z_{\text{abs}} = 3.04954$.

from overlapping absorption by intergalactic gas (see Fig. 7 of Cooke et al. 2011). Consequently, the column density of HI is particularly well determined.

Details of the acquisition and reduction of the spectrum of this QSO can be found in Cooke et al. (2011); here, we summarise the most important points. The spectrum was recorded with the Ultraviolet and Visual Echelle Spectrograph (UVES; Dekker et al. 2000) mounted on UT 2 of the Very Large Telescope facility. The observations were carried out in service mode and consisted of a series of 2700 s exposures; the total integration time was 29 800 s. The echelle spectra were reduced with the standard UVES pipeline and then combined with the software package UVES_POPLER¹ which merges individual echelle orders and maps the data onto a vacuum heliocentric wavelength scale. Flux calibration was achieved by reference to the Sloan Digital Sky Survey spectrum of the QSO.

The final reduced spectrum covers the wavelength range $\lambda_{\text{obs}} = 3710\text{--}6652 \text{ \AA}$ ($\lambda_0 = 916\text{--}1642 \text{ \AA}$ in the rest frame of the DLA) with resolving power $R \simeq 40\,000$ (velocity resolution $\text{FWHM} \simeq 7.5 \text{ km s}^{-1}$) sampled with ~ 3 pixels. The signal-to-noise ratio (S/N) of the data is relatively high considering the magnitude of the source and the high spectral dispersion: $S/N = 43$ at 5000 \AA , and $S/N \geq 20$ over the entire DLA Lyman series (these are values per pixel in the continuum).

Cooke et al. (2011) deduced $\log N(\text{HI})/\text{cm}^{-2} = 20.40 \pm 0.03$. Their analysis of 19 transitions of N I, O I, Si II, and Fe II showed that the metal lines consist of two absorption components of approximately equal optical depth, separated by $\Delta v = 13.8 \text{ km s}^{-1}$ at $z_{\text{abs}} = 3.049649$ and 3.049835 respectively. The Doppler parameters of the two components are $b = 3.5$ and 6.4 km s^{-1} respectively, where $b = \sqrt{2}\sigma$, and σ is the 1-D velocity dispersion of the absorbers projected along

the line of sight. The metallicity of the DLA is approximately 1/100 of solar: $[\text{O}/\text{H}] = -1.92 \pm 0.05$, $[\text{Si}/\text{H}] = -2.08 \pm 0.03$, and $[\text{Fe}/\text{H}] = -2.33 \pm 0.04$ in the usual notation whereby $[\text{X}/\text{H}]_{\text{DLA}} = \log(\text{X}/\text{H})_{\text{DLA}} - \log(\text{X}/\text{H})_{\odot}$. In Fig. 1 we have reproduced examples of the metal lines in the DLA.

3 MEASUREMENT OF D/H

For the reasons outlined above, the spectral characteristics of this DLA are near-ideal for an accurate determination of the D/H ratio and a realistic assessment of its precision. To take advantage of this opportunity, we have performed a detailed spectral analysis in which we identify all of the parameters which potentially affect the derivation of the D/H ratio from the UVES spectrum of J1419+0829, and then use a purpose-built code to solve for all of them simultaneously (via a χ^2 statistic) and thereby deduce the best fitting value of D/H in the DLA. Random and systematic errors affecting this determination were estimated using Monte Carlo techniques. We now discuss the whole procedure in detail.

3.1 QSO continuum

The absorption lines in the DLA are seen against the continuum and emission line radiation from the QSO; the exact level of this flux as a function of wavelength affects directly the measured line optical depths. Reconstruction of the QSO intrinsic spectrum is particularly important for the HI Ly α absorption line which: (i) is blended with the QSO Ly α and N v $\lambda 1240$ emission lines and (ii) affords the best constraint on $N(\text{HI})$. We approximated the QSO flux in the wavelength regions of interest by modelling the QSO intrinsic spectrum with a power-law continuum on which are superimposed a number of emission lines (see Fig. 2). The free parameters that were varied to arrive at the optimum fit (i.e. the fit giving the minimum value of χ^2) are: (i) the slope and (ii) scaling constant of the power-law continuum,

¹ UVES_POPLER is available from http://astronomy.swin.edu.au/~mmurphy/UVES_popler

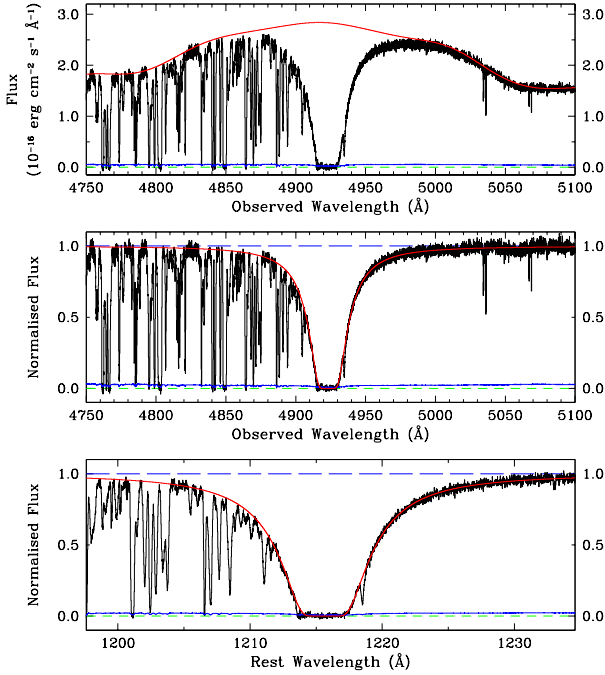


Figure 3. The Ly α region in J1419+0829. *Top panel:* Observed spectrum in black and best-fitting model QSO spectrum in red. *Middle panel:* The normalized spectrum, obtained by dividing the observed spectrum by the model spectrum, is shown in black together with the best fitting damped Ly α absorption profile (see section 3.2) in red. The neutral hydrogen column density is $\log N(\text{H I})/\text{cm}^{-2} = 20.391 \pm 0.008$. *Bottom panel:* Expanded central portion of the middle panel shown in the rest frame of the $z_{\text{abs}} = 3.04984$ DLA. In all three panels the 1σ error spectrum is shown in blue.

and (iii) the redshifts, (iv) amplitudes and (v) widths of the emission lines. Multiplet wavelengths for the emission lines were taken from Morton (2003).

We found that three sets of emission line redshifts were required to reproduce adequately the QSO emission line spectrum: a component at $z_{\text{em}} = 3.04224$ is seen in emission lines of ionised species (C III, C IV, N IV, N V, Si III, Ti III) and in Ly α ; a lower redshift component at $z_{\text{em}} = 2.98576$ further contributes to high ionisation lines (C IV and N V) and to Ly α , while emission lines from low ionisation species (C II, O I, and Si II) are centred at $z_{\text{em}} = 3.04954$. The final fit is shown in red in Fig. 2, where the locations of the different emission line components are colour-coded. The region around Si IV $\lambda 1397$ was not included in the fit because this emission line falls in a gap between the CCD chips on the UVES detector. Fig. 3 shows the region near the Ly α emission+absorption composite before and after division by the QSO flux.

Further fine adjustments were applied to the continuum level in the proximity of the absorption lines to be analysed by fitting low order polynomials to spectral intervals deemed to be free of absorption.

3.2 Absorption lines

Our UVES spectrum of J1419+0829 includes 19 metal absorption lines associated with the $z_{\text{abs}} = 3.04984$ DLA; the

analysis of these features and ensuing abundance determinations have been reported by Cooke et al. (2011). Also covered by our spectrum is the entire Lyman series of the DLA, from Ly α to the Lyman limit. Beyond Ly14 (i.e. for transitions between the ground state and levels with principal quantum number $n > 15$) the line wavelengths differ by $\Delta\lambda_0 < 0.5 \text{ \AA}$ and can no longer be resolved from one another. However, in 8 out of the 14 transitions from Ly α to Ly14, the D I absorption can be separated from the corresponding H I and is clear of other blends (see Fig. 4). The f -values of the transitions in which D I is available for analysis range from 0.013940 (Ly δ) to 0.000469 (Ly14); this factor of ~ 30 spread in line strength provides a wide baseline on the curve of growth for an accurate measurement of $N(\text{D I})$.

3.2.1 Absorption components

While only two absorption components are evident in the metal lines analysed by Cooke et al. (2011; see Fig. 1), an additional, redshifted component was found to contribute to the H I absorption. This component, separated by $+12.7 \text{ km s}^{-1}$ from the redshift of the DLA, has only 3.5×10^{-4} the column density of the DLA, which explains why its presence cannot be discerned in the metal lines (recall that in this DLA $\text{O}/\text{H} \simeq 5 \times 10^{-6}$ and other metals are even less abundant). Even though its contribution to the D I absorption is minimal, this additional component is included in the D I lines by construction since, as explained below, our fitting procedure solves directly for the D I/H I ratio, rather than separately for $N(\text{D I})$ and $N(\text{H I})$ in individual components.

The absorption from each component is characterised by four parameters: (i) redshift z , (ii) column density N , (iii) temperature T , and (iv) large-scale velocity dispersion. The last of these is assumed to be the same for all atoms and ions in the DLA, and is quantified by a turbulent Doppler parameter b_{turb} . On the other hand, a given temperature will correspond to different thermal Doppler parameters for elements of different masses according to the relation $b_{\text{T}}^2 = 2kT/m$ where k is the Boltzmann constant. The two contributions to the line widths add in quadrature: $b_{\text{tot}}^2 = b_{\text{turb}}^2 + b_{\text{T}}^2$. The observation that the two components are unresolved in the D I lines while they are partially resolved in the metal lines (compare Figs. 1 and 4) reflects the larger values of b_{T} for the lighter D compared to the metals, and leads to the conclusion that in this DLA thermal broadening makes a non-negligible contribution to the line width.

Thus, in fitting the absorption line spectrum of the DLA, we varied simultaneously z , N , T , and b_{turb} for each of the two main components of the H I, D I and metal lines. (For the third component seen only in H I we varied z , N , and b_{tot}). The parameters defining the QSO continuum in the proximity of the Ly α emission line were also varied simultaneously to find the set of all of these values which minimises the χ^2 statistic between observed and computed line profiles and the corresponding best-fitting value of D/H .²

² An additional free parameter which was allowed to vary in the χ^2 minimisation procedure is the spectral resolution. The nominal value measured from the widths of emission lines from the Th-Ar lamp used for wavelength calibration is $R \equiv \lambda/\Delta\lambda \simeq 40\,000$.

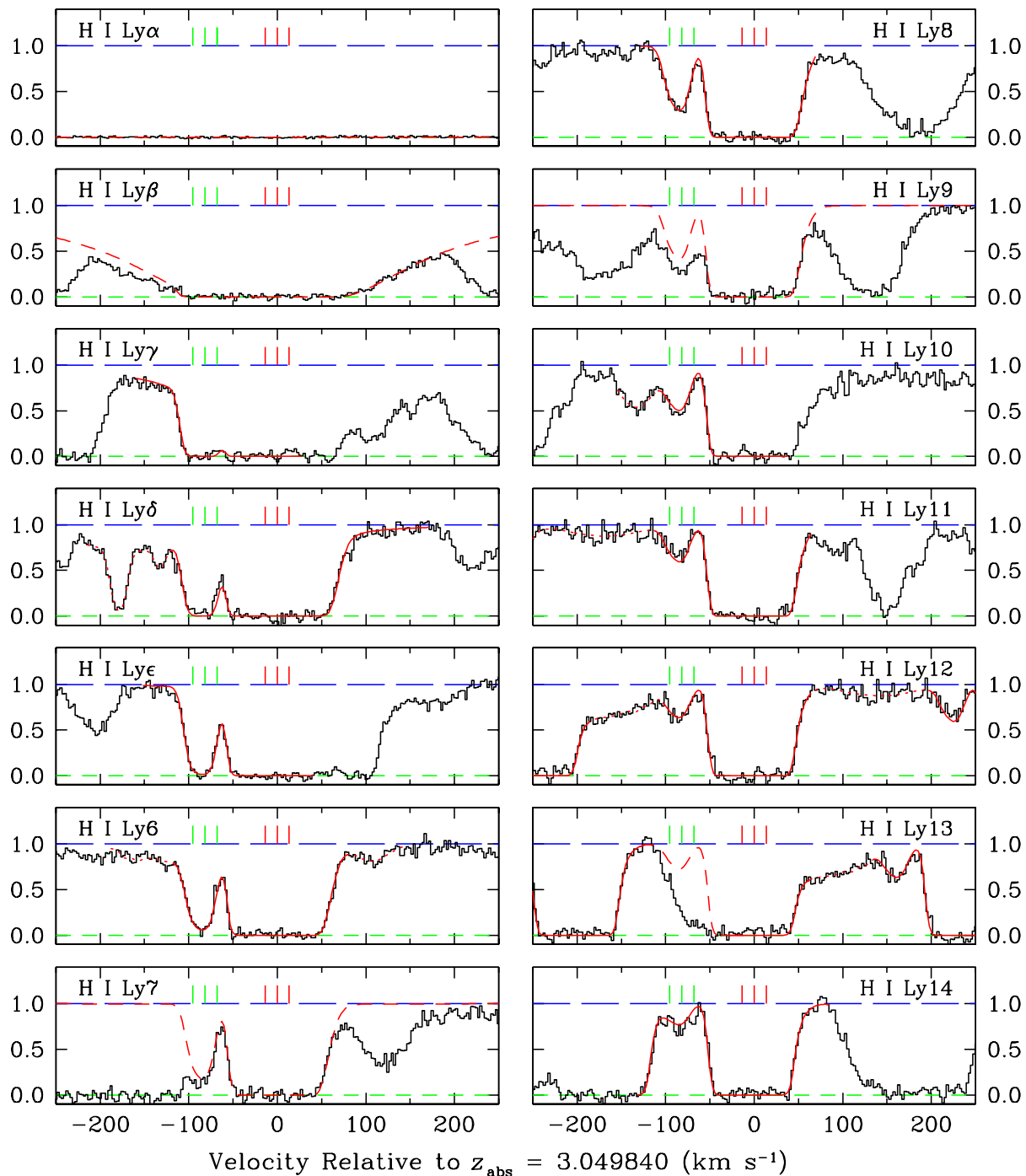


Figure 4. Lyman series lines in the $z_{\text{abs}} = 3.04984$ DLA. Transitions to higher energy levels than Ly14 are too closely spaced in wavelength to be resolved. The black histogram is the observed spectrum, while the red continuous line is the model fit to the absorption features (see section 3.2). Vertical tick marks above the spectrum indicate the three absorption components contributing to the H I (red) and D I (green) absorption. For completeness, we also show (dashed red line) the model H I and D I absorption superposed on blended lines which were *not* used to constrain the model parameters. Dotted red lines are used for fits to features partly blended with D I and H I Lyman lines. In all panels, the y -axis scale is residual intensity.

However, since the spectrograph slit may be illuminated slightly differently by the lamp and the QSO, we preferred to treat the resolution as a free parameter, rather than assuming that it is known perfectly. Reassuringly, the value which was found to fit

It is worth stressing here that this procedure is somewhat different from that adopted in some of the previous

best the shapes of the absorption lines is $R = 39500 \pm 700$, as expected.

Table 1. PARAMETERS OF BEST FITTING ABSORPTION LINE MODEL

Comp.	z_{abs}	T (K)	b_{turb} (km s ⁻¹)	$\log N(\text{H I})$ (cm ⁻²)	$\log(\text{D I}/\text{H I})$	$\log N(\text{N I})$ (cm ⁻²)	$\log N(\text{O I})$ (cm ⁻²)	$\log N(\text{Si II})$ (cm ⁻²)	$\log N(\text{Fe II})$ (cm ⁻²)
1	3.049840 ±0.000002	11 300 ±200	5.3 ±0.2	20.231 ±0.008	-4.601 ^a ±0.008	12.96 ±0.02	14.90 ±0.01	13.595 ±0.009	13.33 ±0.02
2	3.049654 ±0.000001	10 000 ±100	2.3 ±0.2	19.88 ±0.02	-4.601 ^a ±0.008	12.99 ±0.02	14.81 ±0.02	13.52 ±0.02	13.23 ±0.03
3	3.0500 ±0.0001	... ^b	26 ±2	16.9 ±0.3	-4.601 ^a ±0.008	... ^b	... ^b	... ^b	... ^b

^aFixed to be the same in all three components.

^bThe third component is undetected in the metal and D I lines.

derivations of the deuterium abundance. Specifically, in most previous studies of D/H in DLAs, the column densities of H I and D I were determined separately, the former being largely derived from the damping wings of the Ly α line and the latter from the available D I lines in the Lyman series. The ratio of these two column densities then gives D/H. In the present case, by fitting simultaneously all of the H I, D I and metal lines, as well as the QSO flux from which the absorption takes place, we used *all* of the information available in the DLA absorption spectrum to deduce directly the value of D/H (assumed to be the same in all three absorption components) which best fits the data.

In order to fit the data as explained, we developed custom-made software based on the same principles as VPFIT, the software package most commonly used in the analysis of interstellar absorption lines (see <http://www.ast.cam.ac.uk/~rfc/vpfit.html>). Our ABSORPTION LINE FITTING (ALFIT) code, written in the PYTHON programming language, uses a modified version of the MPFIT package (Markwardt 2009).³ MPFIT employs a Levenberg-Marquardt technique to derive the set of model parameters that minimises the χ^2 statistic. We tested ALFIT extensively using fake data with known model parameters, and against VPFIT in simpler cases than that described here, to ensure that its output is fully compatible with that of previous analyses which used VPFIT.

The parameters of the best fitting model are collected in Table 1, and the corresponding line profiles are shown superposed on the observed spectral features in Fig. 4. It is interesting to note that the two components that make up the DLA (components 1 and 2 in Table 1) have temperatures $T \simeq 11\,000$ and $10\,000$ K respectively. A comparably high temperature has been reported recently by Carswell et al. (2012) for a similarly metal-poor DLA, while in other cases somewhat lower temperatures have been inferred (Pettini et al. 2008; Cooke et al. 2012). Temperatures of a few thousand degrees for metal-poor DLAs are consistent with the lack of 21 cm (Srianand et al. 2012; Ellison et al. 2012) and molecular hydrogen (Petitjean et al. 2000) absorption in such systems. We are not able to derive a value of the temperature for component 3 because it is detected only in H I and our method relies on the comparison of the widths of absorption lines from elements of differing masses.

³ MPFIT was originally written for the INTERACTIVE DATA LANGUAGE (IDL) environment and has recently been converted into PYTHON by Mark Rivers and Sergey Koposov.

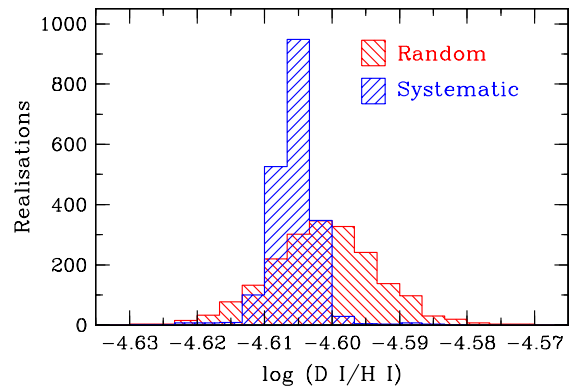


Figure 5. Histograms showing the distribution of values of $\log \text{D I}/\text{H I}$ in 2000 Monte Carlo random realisations of the spectrum of J1419+0829, as described in section 4.

The column densities listed in Table 1 differ by only ~ 0.02 – 0.03 dex from the values reported by Cooke et al. (2011) whose simpler analysis did not differentiate between turbulent and thermal broadening of the absorption lines. For the total neutral hydrogen column density in the DLA we obtain $\log N(\text{H I})/\text{cm}^{-2} = 20.391 \pm 0.008$. The best-fitting value of D/H is $\log(\text{D I}/\text{H I}) = -4.601 \pm 0.008$.

4 ERROR DETERMINATION

An important aspect of the present analysis is an in-depth assessment of the errors, both random and systematic, which apply to the value of D/H deduced above. The first thing to point out is that the errors listed in Table 1 are purely random, reflecting the effect that the 1σ error spectrum has on the derivation of the model parameters; these errors are just the diagonal terms from the covariance matrix.

We tested the validity of this estimate of the random error applicable to the best fitting value of D/H using a suite of simulations, as follows. The parameters defining the best fitting model were used to generate a fake UVES spectrum which was then perturbed by a random realisation of the error spectrum. To ensure that our choice of starting parameters in the line fitting procedure does not bias the result, for each realisation we randomly drew a new set of starting parameters from the covariance array of the best-fitting model that describes the real data. The resulting spectrum was then analysed in an identical manner to the real spec-

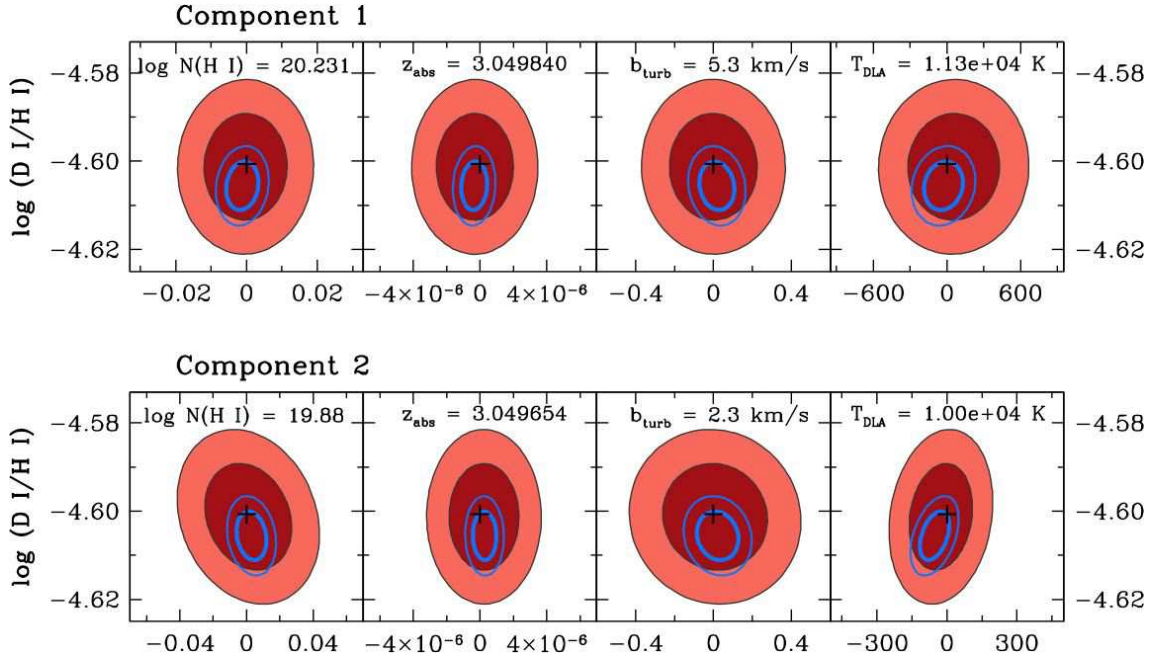


Figure 6. Elliptical contour plots illustrating the covariance between model parameters and the D I/H I ratio. The black cross near the centre of each panel shows the best-fitting value of each parameter, as indicated (see also Table 1), while the x -axis gives the deviation from this value. The red-shaded contours refer to the 1 and 2 σ ranges for the random errors; the corresponding ranges for the systematic errors are shown in blue.

trum (as described in section 3), to derive a new set of best fitting parameters, including the D/H value. This procedure was repeated 2000 times and the distribution of resulting values examined to infer the 1 σ random error on D/H (i.e. the range about the mean encompassing 68% of the 2000 returned values). We found that the error on $\log(D I/H I)$ so derived is $1\sigma_{\text{ran}} = \pm 0.008$ (see Fig. 5), in good agreement with the value obtained from the diagonal terms of the covariance matrix.

The two major sources of systematic error are the continuum placement and the zero level; both affect the measured optical depths of the absorption lines. To assess their impact on the derived value of D/H, we used the above 2000 Monte Carlo realisations and applied continuum and zero level adjustments that reflect the operations performed on the real data. In this way, we can also identify any systematic bias that may be introduced as a result of our continuum and zero level placements.

Examination of the black cores of saturated H I lines of the DLA’s Lyman series indicated that the zero level: (i) is independent of wavelength, and (ii) has an uncertainty of ± 0.0013 (1 σ) of the continuum flux. For the 2000 realisations described above, we perturbed the zero level by a constant amount, drawn at random from a Gaussian distribution of values about zero with a dispersion of 0.0013. The uncertainty resulting from the continuum placement was estimated by repeating the same fine continuum adjustments described in section 3.1 on each of the 2000 randomly generated spectra and redetermining the best fitting model parameters as before.

For each realisation, we take the difference between the best-fitting value of D/H, respectively with and without the aforementioned corrections, as an indication of the system-

atic uncertainty affecting the derivation of the D/H ratio. The distribution of such differences in the 2000 trials then gives the estimate of the systematic error and bias in our measure of $\log(D I/H I)$.

As can be seen from Fig. 5, this second set of tests indicates that: (i) the magnitude of the systematic error is small: $1\sigma_{\text{sys}} = \pm 0.003$; and (ii) there appears to be a bias of -0.005 in our estimate of $\log(D I/H I)$ introduced by a (small) error in the continuum placement. A further advantage of our approach is that it allows us to examine in detail the sensitivity of the D/H ratio to each of the model parameters entering in its derivation. In Fig. 6 we have reproduced some examples; the error contours are ‘well-behaved’ and we see only mild correlations between D I/H I and some of the model parameters.

The result of all of the above tests is as follows:

$$\log(D I/H I) = -4.596 \pm 0.008 \pm 0.003 \quad (1)$$

(random and systematic 1 σ errors respectively), which includes the correction of $+0.005$ dex for the bias in the continuum and zero level placement.

Combining the two errors in quadrature, leads to:

$$\log(D I/H I) = -4.596 \pm 0.009, \quad (2)$$

or:

$$10^5(D I/H I) = 2.535 \pm 0.05. \quad (3)$$

5 COSMOLOGICAL IMPLICATIONS

Our determination of D/H in J1419+0829 is more precise than those reported up to now in other QSO absorbers for the following reasons: (i) The red wing of the damped Ly α

line suffers very little contamination by gas unrelated to the DLA, easing the determination of $N(\text{H I})$; (ii) eight D I Lyman lines of widely differing f -values are accessible; (iii) the kinematic structure of the gas is simple, with only 2–3 components contributing to the absorption lines; and (iv) the spectrum analysed is of moderately high S/N. We therefore consider it worthwhile to examine the cosmological implications of the new measurement reported here before discussing the full sample of available D/H measures at high redshift.

In the following, we take:

$$(\text{D I}/\text{H I})_{\text{DLA}} = (\text{D}/\text{H})_{\text{DLA}} = (\text{D}/\text{H})_{\text{p}}. \quad (4)$$

The assumptions underlying these equalities are that: (i) the fractional ionizations of H and D are the same, (ii) D is not depleted relative to H, and (iii) the destruction of D through astration prior to the time when we observe the DLA has been negligible. Concerning the first assumption, we are not aware of a physical process that would under- or over-ionise one isotope relative to the other. Dust depletion of D in the local interstellar medium has been proposed to explain the surprising range of D/H values found along different sightlines in our Galaxy (Linsky et al. 2006), but is unlikely to be important in metal- and dust-poor DLAs where even highly refractory elements are present in near-solar relative proportions (Akerman et al. 2005; Vladilo et al. 2006; Ellison et al. 2007). Given the low metallicity of the $z_{\text{abs}} = 3.04984$ DLA, where N, O, Si, and Fe have abundances less than $\sim 1/100$ of solar (Cooke et al. 2011), the third assumption is supported by chemical evolution models which entertain little reduction of the D abundance from its primordial value when such a small fraction of the gas has evidently been cycled through stars (Romano et al. 2006).

Recently, Steigman (private communication) has updated the relations between $(\text{D}/\text{H})_{\text{p}}$ and $\Omega_{\text{b},0}h^2$ given by Simha & Steigman (2008) and Steigman (2007), as follows:

$$10^5 (\text{D}/\text{H}) = 2.60(1 \pm 0.06) \left[\frac{6}{\eta_{10} - 6(S - 1)} \right]^{1.6}, \quad (5)$$

where η_{10} is the post- e^{\pm} annihilation ratio of the numbers of baryons and photons in units of 10^{-10} :

$$\eta_{10} \equiv 10^{10} n_{\text{b}}/n_{\gamma} = 273.9 \Omega_{\text{b},0} h^2, \quad (6)$$

and S is the non-standard expansion rate factor, related to the number of additional (equivalent) neutrinos $\Delta N_{\nu} \equiv N_{\nu} - 3$ by:

$$S^2 \equiv \left(\frac{H'}{H} \right)^2 = 1 + \frac{7\Delta N_{\nu}}{43} \quad (7)$$

The 6% error in the conversion factor in eq. (5) reflects the uncertainties in the nuclear reaction rates, particularly the $d(p, \gamma)^3\text{He}$ cross-section (e.g. Nollett & Holder 2011), used in BBN codes (Steigman, private communication).

For standard BBN with $S = 1$, eqs. (3), (5), and (6) yield:

$$100\Omega_{\text{b},0}h^2(\text{BBN}) = 2.23 \pm 0.03 \pm 0.08 \quad (8)$$

where the error terms reflect the uncertainties in, respectively, $(\text{D}/\text{H})_{\text{p}}$ (eq. 3) and BBN calculations (eq. 5). Combining the two error terms in quadrature, we have:

$$100\Omega_{\text{b},0}h^2(\text{BBN}) = 2.23 \pm 0.09. \quad (9)$$

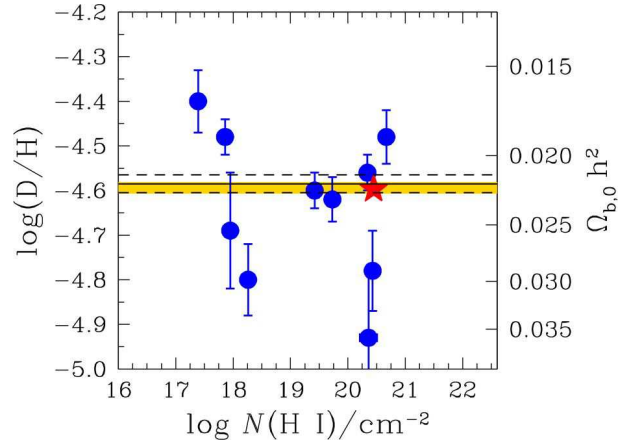


Figure 7. Measures of the deuterium abundance in high redshift QSO absorbers. Only cases where the deuterium absorption is clearly resolved from nearby spectral features are shown (see text). The red star refers to the new measurement reported here, with errors smaller than the symbol size. The horizontal lines are drawn at the weighted mean value of $\log(\text{D}/\text{H})$ and its error, as determined with the bootstrap method. The yellow shaded area shows the range in $\Omega_{\text{b},0}h^2(\text{CMB})$ from Keisler et al. (2011).

Recently, Keisler et al. (2011) combined their measurement of the CMB angular power spectrum from the South Pole Telescope (SPT) with the power spectra from the seven-year Wilkinson Microwave Anisotropy Probe (WMAP) data release to better constrain cosmological parameters. From this analysis, it was concluded:

$$100\Omega_{\text{b},0}h^2(\text{CMB}) = 2.22 \pm 0.042 \quad (10)$$

(see Table 3 of Keisler et al. 2011).

The agreement between eqs. (9) and (10) is very encouraging. If the value of $(\text{D}/\text{H})_{\text{p}}$ we have deduced here is indeed the correct one, there may be no need to appeal to non-standard physics to reconcile BBN and CMB estimates of $\Omega_{\text{b},0}$ (see, for example, the discussion of this point by Hamann et al. 2011). Specifically, if we adopt the value $100\Omega_{\text{b},0}h^2(\text{CMB}) = 2.22 \pm 0.042$ from Keisler et al. (2011) and then use eqs. (5), (6), and (7) to solve for ΔN_{ν} using the determination of $(\text{D}/\text{H})_{\text{p}}$ reported here (eq. 3), we find:

$$N_{\nu} = 3.0 \pm 0.5 \quad (11)$$

combining in quadrature the errors on $(\text{D}/\text{H})_{\text{p}}$, BBN reaction rates and $\Omega_{\text{b},0}h^2(\text{CMB})$, with the BBN rates making the largest contribution to the total uncertainty. This value is in good agreement with $N_{\nu} = 2.984 \pm 0.008$ deduced from the width of Z-boson decays in electron-positron colliders (ALEPH Collaboration et al. 2006).

6 COMPARISON WITH OTHER MEASUREMENTS OF D/H

In the previous section, we used our new, precise measure of D/H to compare the present day baryon density derived from BBN calculations and CMB measurements. However, a full comparison between $\Omega_{\text{b},0}(\text{BBN})$ and $\Omega_{\text{b},0}(\text{CMB})$ should include all reliable measurements of the primordial abundances of the light elements created in BBN. It is beyond

Table 2. PRIME SAMPLE OF D/H MEASUREMENTS IN QSO ABSORPTION LINE SYSTEMS

QSO	z_{em}	z_{abs}	$\log N(\text{H I})$ (cm^{-2})	[O/H] ^a	$\log(\text{D}/\text{H})$	Ref. ^b
HS 0105+1619	2.640	2.53600	19.42 ± 0.01	-1.73	-4.60 ± 0.04	1
Q0913+072	2.785	2.61843	20.34 ± 0.04	-2.40	-4.56 ± 0.04	2, 3
Q1009+299	2.640	2.50357	17.39 ± 0.06	$< -0.70^{\text{c}}$	-4.40 ± 0.07	4
SDSS J1134+5742	3.522	3.41088	17.95 ± 0.05	$< -1.9^{\text{d}}$	-4.69 ± 0.13	5
Q1243+307	2.558	2.52566	19.73 ± 0.04	-2.79	-4.62 ± 0.05	6
SDSS J1337+3152	3.174	3.16768	20.41 ± 0.15	-2.68	-4.93 ± 0.15	7
SDSS J1419+0829	3.030	3.04984	20.391 ± 0.008	-1.92	-4.596 ± 0.009	8, 9
SDSS J1558-0031	2.823	2.70262	20.67 ± 0.05	-1.50	-4.48 ± 0.06	10
Q1937-101	3.787	3.25601	18.26 ± 0.02	-2.0 ^e	-4.80 ± 0.08	11
Q1937-101	3.787	3.57220	17.86 ± 0.02	< -0.9	-4.48 ± 0.04	12
Q2206-199	2.559	2.07624	20.43 ± 0.04	-2.07	-4.78 ± 0.09	2, 13

^aRelative to the solar value $\log(\text{O}/\text{H})_{\odot} + 12 = 8.69$ (Asplund et al. 2009).

^bReferences – (1) O’Meara et al. (2001), (2) Pettini et al. (2008a), (3) Pettini et al. (2008b), (4) Burles & Tytler (1998b), (5) Fumagalli et al. (2011), (6) Kirkman et al. (2003), (7) Srianand et al. (2010), (8) This work, (9) Cooke et al. (2011), (10) O’Meara et al. (2006), (11) Crighton et al. (2004), (12) Burles & Tytler (1998a), (13) Pettini & Bowen (2001).

^cThis is a very conservative upper limit on the metallicity. Burles & Tytler (1998b) estimate $[\text{Si}/\text{H}] \simeq -2.5$ and $[\text{C}/\text{H}] \simeq -2.9$ from photoionisation modelling.

^dThis is a conservative upper limit on the metallicity. Fumagalli et al. (2011) estimate $[\text{Si}/\text{H}] \simeq -4.2$ from photoionisation modelling.

^eThis value refers to $[\text{Si}/\text{H}]$ as the O abundance was not measured by Crighton et al. (2004).

the scope of this paper to comment on the difficulties in deducing the primordial abundances of ^4He and ^7Li from, respectively, the emission line spectra of metal-poor H II regions and the absorption spectra of some of the oldest stars in the Galaxy. We refer the interested reader to the review by Steigman (2007) for a detailed discussion.

Here, we focus specifically on the derivation of $(\text{D}/\text{H})_{\text{p}}$. Since the compilation assembled by Pettini et al. (2008), two new measurements of $(\text{D}/\text{H})_{\text{p}}$ have been reported, by Srianand et al. (2010) and Fumagalli et al. (2011). In the former case, the D I lines are only partially resolved from nearby blends, so that its inclusion in what we consider to be the most reliable set of measurements is questionable but, for completeness, we have included this DLA in the sample. Together with the new detection reported here, the full data set now consists of 11 measurements of $(\text{D}/\text{H})_{\text{p}}$ whose main characteristics are collected in Table 2.

As can be seen from Fig. 7, there is a troublesome dispersion between the 11 measurements, well in excess of the quoted errors. The problem is that even this set is highly heterogeneous. The number of D I Lyman lines covered varies between the 11 QSO absorbers, with only Ly α and Ly β available in systems of lower $N(\text{H I})$. The degree of line blending is significantly worse in some cases than in others. Some spectra are of inferior S/N ratio than others, such as that of the $z_{\text{abs}} = 2.07624$ DLA in Q2206-199 which, because of the lower redshift of this absorber, necessitated observations at ultraviolet wavelengths with the *Hubble Space Telescope* (Pettini & Bowen 2001). Perhaps most importantly, the efforts devoted to evaluating realistic errors vary considerably between the different analyses collected in Table 2, and we suspect that in at least some cases the errors quoted may well be underestimates, and the values reported may suffer from biases that are unaccounted for.

It is our contention that the only way forward with this problem is to assemble a uniform sample of metal-poor DLAs, observed at comparable S/N, and analysed consistently following procedures similar to those employed here. Unfortunately, this ambitious goal is still some way off in the future. Given the reservations expressed above, it is unclear to the present authors whether there is much to be learnt by averaging the measurements in Table 2. Nevertheless, for completeness, we have estimated the mean $\langle(\text{D}/\text{H})_{\text{p}}\rangle$ using the bootstrap method. That is, we calculated the weighted mean of the 11 measurements in Table 2 adopting the errors quoted in the original reports, and repeated the calculation 10000 times by random sampling (with substitution) of the 11 values of $(\text{D}/\text{H})_{\text{p}}$. The mean and standard deviation of the results of 10000 such trials are:

$$\langle\log(\text{D}/\text{H})_{\text{p}}\rangle = -4.585 \pm 0.02. \quad (12)$$

For comparison, Fumagalli et al. (2011) calculated $\langle\log(\text{D}/\text{H})_{\text{p}}\rangle = -4.556 \pm 0.034$, while Pettini et al. (2008) reported $\langle\log(\text{D}/\text{H})_{\text{p}}\rangle = -4.55 \pm 0.03$; both estimates are from subsets of the data in Table 2. Thus, the new case highlighted here has reduced slightly both the mean of the sample and its error, but the main conclusion is that the value of $\langle\log(\text{D}/\text{H})_{\text{p}}\rangle$ has remained relatively stable over the last few years.

7 SUMMARY AND CONCLUSIONS

In summary, we have identified a metal-poor DLA from the recent survey of such systems by Cooke et al. (2011) with near-ideal properties for an accurate determination of the primordial abundance of deuterium. To capitalise on this rare opportunity, we have developed a spectral analysis specifically targeted at finding the most likely value of

D/H by varying all of the spectral parameters which have a bearing on this measurement. We have also paid particular attention to the assessment of the errors and biases, both random and systematic, which affect our determination of D/H.

Our principal result is that the value of $(D/H)_p$ so derived, $(D/H)_p = (2.535 \pm 0.05) \times 10^{-5}$, implies $\Omega_{b,0} h^2 = 0.0223 \pm 0.0009$ which is in excellent agreement with $\Omega_{b,0} h^2(\text{CMB}) = 0.0222 \pm 0.0004$ deduced from the joint analysis of the CMB angular power spectrum recorded with the WMAP and SPT experiments. On the basis of the new measurement reported here, there is no need to invoke non-standard physics, nor appeal to early astration of deuterium, to reconcile CMB and D/H determinations of the cosmic density of baryons.

When considered in the context of previous reports of D/H values in QSO absorbers, the new case presented in this paper highlights the heterogeneity of the existing data set. The weighted mean of what are often considered to be the best 11 available measurements is $\langle (D/H)_p \rangle = (2.6 \pm 0.1) \times 10^{-5}$, but it is hard to assess the significance of this mean value when it is likely that systematic errors and biases may have been overlooked in at least some earlier analyses.

Looking ahead, we can expect a further refinement in the determination of $\Omega_{b,0} h^2(\text{CMB})$ from the Planck mission (Planck Collaboration et al. 2011). However, improvements in the value of $(D/H)_p$ made possible by the identification and careful analysis of suitable metal-poor DLAs remain a priority, given their potential for clarifying our understanding of primordial nucleosynthesis (including the relevant nuclear reaction rates) and of the subsequent processing of ^4He and ^7Li . As an added bonus, more detections of D I absorption in metal-poor DLAs will increase the limited statistics on the kinetic temperature of these structures and help us isolate the dominant physical processes that regulate it.

ACKNOWLEDGEMENTS

We are grateful to the ESO time assignment committee for their continuing support of this demanding observational programme, and to the staff astronomers at Paranal who conducted the observations. It is a pleasure to acknowledge helpful and stimulating conversations with Bob Carswell, Dawn Erb, Jan Hamann, Paul Hewett, Mike Irwin, Lloyd Knox, Michael Murphy, Subir Sarkar, and Gary Steigman. We are grateful to Gary Steigman for communicating his revised fitting formulae in advance of publication, and to the referee, John Webb, for valuable comments which improved the paper.

REFERENCES

- Adams T. F. 1976, *A&A*, 50, 461
 Akerman, C. J. Ellison S. L., Pettini M., Steidel C. C. 2005, *A&A*, 440, 499
 ALEPH Collaboration, DELPHI Collaboration, L3 Collaboration, et al. 2006, *Phys. Rep.*, 427, 257
 Asplund M., Grevesse N., Sauval A. J., Scott, P., 2009, *ARA&A*, 47, 481
 Aver E., Olive K. A., Skillman E. D. 2012, *JCAP*, 4, 4
 Burles S., Tytler D. 1998a, *ApJ*, 499, 699
 Burles S., Tytler D. 1998b, *ApJ*, 507, 732
 Carswell R. F., Becker G. D., Jorgenson R. A., Murphy M. T., Wolfe A. M. 2012, *MNRAS*, 422, 1700
 Cooke R., Pettini M., Steidel C. C., Rudie G. C., Nissen P. E. 2011, *MNRAS*, 417, 1534
 Cooke R., Pettini M., Murphy M. 2012, *MNRAS*, in press (arXiv:1201.1004)
 Dekker H., D'Odorico S., Kaufer A., Delabre B., Kotzlwski H., 2000, *SPIE*, 4008, 534
 Ellison S. L., Prochaska J. X., Lopez S. 2007, *MNRAS*, 380, 1245
 Ellison S. L., Kanekar N., Prochaska J. X., Momjian E., Worseck G., 2012, *MNRAS*, submitted
 Fumagalli M., O'Meara J. M., Prochaska, J.X. 2011, *Science*, 334, 1245
 Hamann J., Hannestad S., Raffelt, G. G. Wong Y. Y. Y. 2011, *JCAP*, 9, 34
 Iocco, F. 2012, *Mem. S.A.It.*, in press (arXiv:1206.2396)
 Keisler R., Reichardt C. L., Aird K. A., et al. 2011, *ApJ*, 743, 28
 Kirkman D., Tytler D, Suzuki N., O'Meara J. M., Lubin D. 2003, *ApJS*, 149, 1
 Krogager J.-K., Fynbo J. P. U., Møller P., et al. 2012, *MNRAS*, in press (arXiv:1204.2833)
 Linsky J. L., Draine B. T., Moos H. W., et al. 2006, *ApJ*, 647, 1106
 Markwardt C. B., 2009, *ASPC*, 411, 251
 Molaro, P. 2008, in Knapen J. H., Mahoney T. J., Vazdekis A., eds, *ASP Conf. Ser. Vol. 390, Pathways Through an Eclectic Universe*, Astron. Soc. Pac., San Francisco, p. 472
 Morton, D. C. 2003, *ApJS*, 149, 205
 Murphy M. T., Curran S. J., Webb J. K., Ménager H., Zych B. J. 2007, *MNRAS*, 376, 673
 Nissen P. E., Schuster W. J. 2012, *A&A*, 543, A28
 Nollett K. M., Holder G. P. 2011, *Phys. Rev. D*, submitted (arXiv:1112.2683)
 Noterdaeme P., Petitjean P., Ledoux C., Srianand R. 2009, *A&A*, 505, 1087
 Olive K. A., Petitjean P., Vangioni E., Silk J. 2012, arXiv:1203.5701
 O'Meara J. M., Burles S., Prochaska J.X., Prochter G. E. 2006, *ApJ*, 649, L61
 O'Meara J. M., Tytler D., Kirkman D., Suzuki N., Prochaska J.X., Lubin D., Wolfe A. M. 2001, *ApJ*, 552, 718
 Penprase B. E., Prochaska J. X., Sargent W. L. W., Toromartinez I., Beeler D. J. 2010, *ApJ*, 721, 1
 Péroux C., Bouché N., Kulkarni V. P., York D. G., Vladilo G. 2012, *MNRAS*, 419, 3060
 Petitjean P., Srianand R., & Ledoux C. 2000, *A&A*, 364, L26
 Pettini M., Bowen D. V. 2001, *ApJ*, 560, 41
 Pettini M., Zych B. J., Steidel C. C., Chaffee F. H. 2008a, *MNRAS*, 385, 2011
 Pettini M., Zych B. J., Murphy M. T., Lewis A., Steidel C. C. 2008b, *MNRAS*, 391, 1499
 Planck Collaboration, Ade P. A. R., Aghanim N., et al. 2011, *A&A*, 536, A1
 Pontzen A., Governato F., Pettini M., et al. 2008, *MNRAS*, 390, 1349
 Prochaska J. X., Chen H.-W., Wolfe A. M., Dessauges-Zavadsky M., Bloom J. S. 2008, *ApJ*, 672, 59
 Prodanović T., Steigman G., Fields B. D. 2010, *MNRAS*, 406, 1108
 Romano D., Tosi M., Chiappini C., Matteucci F. 2006, *MNRAS*, 369, 295
 Sbordone L., Bonifacio P., Caffau E., et al. 2010, *A&A*, 522, A26
 Simha V., & Steigman G. 2008, *JCAP*, 6, 16
 Srianand R., Gupta N., Petitjean P., Noterdaeme P., Ledoux,

- C. 2010, MNRAS, 405, 1888
Srianand R., Gupta N., Petitjean P., et al. 2012, MNRAS, 421, 651
Steigman G. 2007, Annual Review of Nuclear and Particle Science, 57, 463
Vladilo G., Centurión M., Levshakov S. A., et al. 2006, A&A, 454, 151
Wolfe A. M., Gawiser E., Prochaska J. X. 2005, ARA&A, 43, 861